Photonic Sensors (2013) Vol. 3, No. 1: 44–51

DOI: 10.1007/s13320-012-0089-9 **Photonic Sensors**

Regular

Fiber Laser Sensor Based on a Phase-Shifted Chirped Grating for Acoustic Sensing of Partial Discharges

Sanderson E. U. LIMA[1], Rubem G. FARIAS[2], Francisco M. ARAÚJO[1], Luís A. FERREIRA[1], José L. SANTOS[1,3], Vladimiro MIRANDA[1,4], and Orlando FRAZÃO[1*]

[1]*INESC Porto, Rua do Campo Alegre, 687, Porto 4169-007, Portugal*

[2]*Faculdade de Engenharia da Computação, Universidade Federal do Pará, Belém, Brasil*

[3]*Faculdade de Ciências da Universidade do Porto, Rua do Campo Alegre, 687, Porto 4169-007, Portugal*

[4]*Faculdade de Engenharia da Universidade do Porto, Rua Dr. Roberto Frias, s/n, Porto 4200-465,Portugal*

[*]Corresponding author: Orlando FRAZÃO E-mail: ofrazao@fc.up.pt

Abstract: Acoustic emission monitoring is often used in the diagnosis of electrical and mechanical incipient faults in the high voltage apparatus. Partial discharges are a major source of insulation failure in electric power transformers, and the differentiation from other sources of acoustic emission is of the utmost importance. This paper reports the development of a new sensor concept – a fiber laser sensor based on a phase-shifted chirped fiber grating – for the acoustic emission detection of incipient faults in oil-filled power transformers. These sensors can be placed in the inner surface of the transformer tank wall, not affecting the insulation integrity of the structure and improving fault detection and location. The performance of the sensing head is characterized and compared for different surrounding media: air, water, and oil. The results obtained indicate the feasibility of this sensing approach for the industrial development of practical solutions.

Keywords: Transformer insulation, partial discharges, acoustic detection, fiber laser sensors

Citation: Sanderson E. U. LIMA, Rubem G. FARIAS, Francisco M. ARAÚJO, Luís A. FERREIRA, José L. SANTOS, Vladimiro MIRANDA, *et al*., "Fiber Laser Sensor Based on a Phase-Shifted Chirped Grating for Acoustic Sensing of Partial Discharges," *Photonic Sensors*, vol. 3, no. 1, pp. 44–51, 2013.

1. Introduction

Fiber sensors are used in power transformers to detect acoustic emissions (AE) that are generated by electrical and mechanical sources [1]. It is possible to identify the AE source using the characteristic signature of each emission; indeed, from this signature emission parameters such as the burst rate and count rate can be evaluated and compared with those derived from known AE sources [2].

The levels of partial discharges (PDs) are indicators of the insulation condition of a transformer because they result from the localized electrical breakdown that should not be present in significant values in a good insulation system. PDs are pulse-like in nature, and its acoustic detection is based on the mechanical pressure wave emitted from the discharge [3]. These waves propagate within the transformer throughout the surrounding oil and hit the transformer tank wall. The accuracy of the PD detection and location can be improved using optical fiber sensors that can be placed inside the transformer tank without affecting the insulation integrity.

Received: 31 July 2012 / Revised version: 12 August 2012

Acoustic sensing has been one of the first successful applications of fiber optic sensors [4, 5]. Early, fiber laser sensors based on FBGs were implemented using Fabry-Peròt resonators [6, 7]. These sensors showed the improved sensitivity, gaining the advantage from their reduced linewidth which made them a frequency discriminator better than a simple FBG sensor. Fiber Bragg lasers have demonstrated the sensitivity at the level of few tens of femto-strain for signals in the kilohertz bandwidth, and their potentiality as acoustic sensors in water has already been exploited up to 100 kHz [8–10]. Erbium-doped fiber ring lasers (EDFRLs) have recently attracted great interest due to such promising applications as optical sensors. The EDFRLs have advantages which include high output power, low intensity noise, and compatibility with fiber components [11–15]. Recently, EDFRLs using the phase-shifted linearly chirped FBG (PS-LCFBG) were reported [16]. This laser configuration had a simple all-fiber structure and is cost-effective for use in applications as optical sensing.

With the intrinsic advantages of fiber optics sensors in mind, this paper describes the development of a fiber laser sensor based on a phase-shifted chirped fiber grating for detection of acoustic emission with characteristics adapted to utilization in power transformers. A device of this type was attached to a compliant mandrel with its wall vibrating in the presence of an acoustic wave. A Mach-Zehnder interferometer was used to interrogate the sensing head, and a feedback loop, in a homodyne configuration, tracked the quadrature point, optimizing the measurand readout sensitivity. The experimental tests described the use of acoustic transducers under a concept that better suited the objectives looked for, i.e., it was not used “artificial” PD sources (e.g. rod-plates electrodes), because they could not reproduce accurately the real characteristics of PDs in transformers (energy intensity, number of charges, frequency content, spark signature, etc). Instead, data have been collected from literature (front wave pressure, duration, frequency content, repetition rate, etc), which allowed the reproduction of acoustic waves that were generated by partial discharges. This procedure, from the acoustic point of view, could be the most reliable way to reproduce, in the lab, the main characteristics of a real PD occurrence. The distance, angular and frequency responses, as well as the device sensitivity, were experimentally obtained, and the effects on the characteristics of the sensing head when it was immersed in different fluids (air, water and oil) were addressed. Future research paths are summarized in the last section.

2. Sensing head

The sensing head used a phase-shifted chirped fiber Bragg grating (PS-CFBG) to detect acoustic waves. With this sensing element, the sensitivity depended on the amount of energy that was transferred from a pressure wave to the core of the fiber optic (inducing a strain along the axes), producing, therefore, a shift in the Bragg wavelength. An acoustic amplifier (mandrel) was used in order to improve the interaction area between the incident pressure wave and the fiber optics, and its project was optimized for detecting the presence of the ultrasonic components of acoustic emission. Figure 1 shows the wave shape of a real PD acoustic signal (a) in the time domain and (b) in the frequency domain. The acoustic emission of PDs had the wideband frequency content (10 kHz to 500 kHz), but considering the attenuation and the energy density, and a sensor with a response in the frequency range of 50 kHz to 200 kHz was considered as a good acoustic PD detector [17]. Also, considering the high stiffness of the fiber optic material, it was realized that the acoustically induced wavelength shifts were small, thus a high-resolution interrogation system

was necessary to demodulate the optical signal.

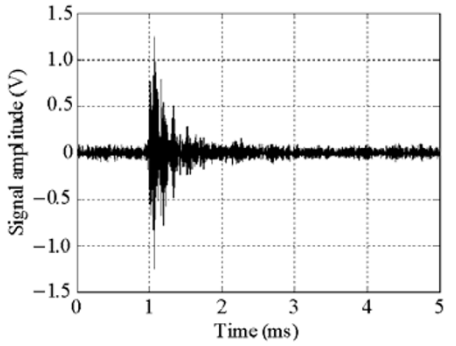

(a)

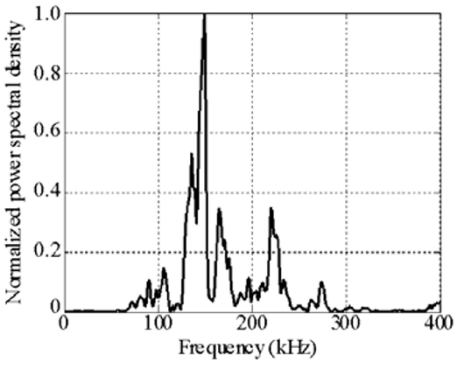

(b)

Fig. 1 Acoustic emission impulse detected by a piezoelectric sensor close to a real PD source: (a) in the time domain and (b) in the frequency domain.

2.1 Mathematical vibration model of the mandrel

A theoretical evaluation was done using the mathematical model for a thin walled cylinder to obtain the displacement values in the axial and radial directions in terms of n (the nodes of circumferential waves) and m (the number of axial half-periods). From such model, the resonances frequencies are given by [18, 19]

$$\omega_{m,n}^2 = \frac{E}{\rho(1-\upsilon^2)R^2}\left(\frac{(1-\upsilon^2)\lambda^4 + a^2(\lambda^2+n^2)^4}{n^2+(\lambda^2+n^2)^2}\right) \quad (1)$$

where E is the Young modulus, υ is the Poisson ratio, ρ is the material density, R, L and t are, respectively, the radius, length and thickness of the cylinder, $\lambda = (m\pi R)/L$ and

$$a^2 = \frac{t^2}{12R^2}. \quad (2)$$

For the present application, it is relevant to determine the values of m and n for which the smallest natural frequency of predominantly transverse vibration occurs. This condition is obtained for m=1 and n is a nearest integer from n':

$$n' = \left[\lambda.\left(\left(\frac{(1-\upsilon^2)}{a^2}\right)^{1/4} - \lambda\right)\right]^{1/2}. \quad (3)$$

Another important normal mode, which affects more directly the response of the fiber attached circumferentially, is the "breathing" mode with n=0 and m=1. The fundamental modal frequency resonance ($\omega_{1,0}$) associated with this pure radial motion that corresponds to extensional vibrations is

$$\omega_{1,0}^2 = \frac{E}{\rho(1-\upsilon^2)R^2}\left[(1-\upsilon^2) + \frac{t^2\pi^4R^2}{12L^4}\right]. \quad (4)$$

If the mandrel is immersed in a fluid, in general the resonance frequency will lower due to the added mass effect, and it will also decrease the amplitude at the peak due to re-radiation of the acoustic energy [14]. The response is expressed as the normalized radial displacement, $W_{1,0}(\omega)/R$, produced by a pressure wave Δp of the frequency ω:

$$\frac{W_{1,0}(\omega)}{R} = \Delta p_\omega \frac{R(1-\upsilon^2)}{Et}\frac{1}{\left(\frac{\rho_0(1-\upsilon^2)R^2\omega^2}{E}\right)} \cdot \frac{1}{\left(1+\frac{\rho_0}{\rho_1}\frac{K_0(\gamma R)}{\gamma K_1(\gamma R)}\right) - 1 - \frac{t^2\pi^4R^2}{12L}} \quad (5)$$

where ρ_0, ρ_1 are the air and fluid densities, $K_0(\gamma R)$, $K_1(\gamma R)$ are the modified Bessel functions of order zero and one, and

$$\gamma^2 = \frac{\pi^2}{L^2} - \frac{\omega^2}{v_l^2} \quad (6)$$

where v_l is the sound velocity of the fluid, and γ is imaginary value for frequency f above $v_l/2L$, indicating that the cylinder is reinforcing the sound wave [20].

The sensor was designed to monitor acoustic emission inside a transformer. Thus, the materials to be used for its fabrication must be dielectrics to

avoid problems with the insulation system. A relatively flat frequency response in the range of 50 kHz–200 kHz was also desirable. In view of these requirements and using the above equations, the mandrel was designed as a cylinder of polycarbonate, 20 mm long, with an outer diameter of 10 mm and a thickness of 0.5 mm.

2.2 Sensor configuration

The experimental setup is shown in Fig. 2. The sensing head had a compliant mandrel as a transducer element. The mandrel's wall vibrated in the presence of an acoustic wave and transferred a pressure wave to the fiber sensing element. The

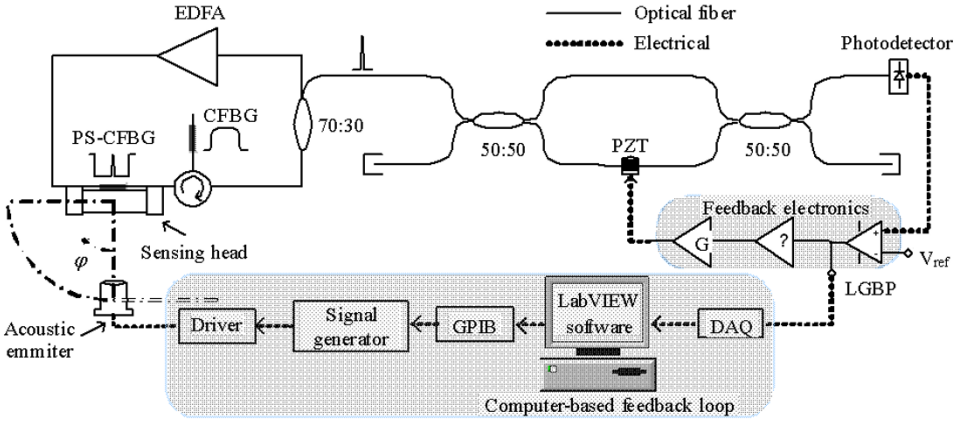

Fig. 2 Experimental setup: sensing head configuration, interrogation system, feedback electronics, computer-based data acquisition and signal generator.

optical elements of the sensing head consisted of a PS-CFBG, a CFBG (which was identical to the PS-CFBG but without the central transmission window), a circulator, an erbium-doped fiber amplifier (EDFA) and an optical coupler (70:30). These optical components were arranged in order to form a ring laser. The PS-CFBG had a narrow passband peak with a bandwidth of 20 pm at –3 dB (the transmission spectrum is shown in the Fig. 3). The CFBG was used to suppress the unwanted laser output outside the stopband of the transmissive

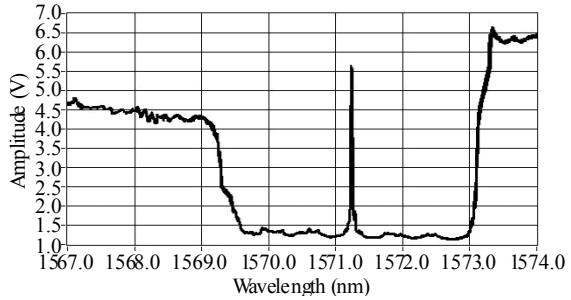

Fig. 3 Transmission spectrum of the PS-CFBG that is used as a sensing element.

PS-CFBG, allowing stable laser operation to be achieved. The lasing wavelength (the laser linewidth coincided with the center of the transmissive PS-CFBG) was dynamically changed by the pressure wave that induced a phase shift into the PS-CFBG. Figure 4 shows a close-up view of the ultra-narrow laser linewidth obtained with the Advantest® 8384, a high resolution optical spectral analyzer (OSA). The sensor was interrogated by a Mach-Zehnder interferometer with a path imbalance of 1 mm. The active homodyne stabilization was used in order to obtain a linear relationship between the Bragg wavelength shift and the electrical output signal. The stabilization feedback loop included a piezoelectric transducer (PZT) where an electrical signal was applied as the necessary signal and amplitude to maintain the interferometer locked at the quadrature condition (the highest sensitivity point) in order to compensate the temperature fluctuations. The stored data were the fast Fourier transform (FFT) of the time domain low

gain-bandwidth product (LGBP) signal. Figure 5 shows the FFT output signal of the LGBP signal.

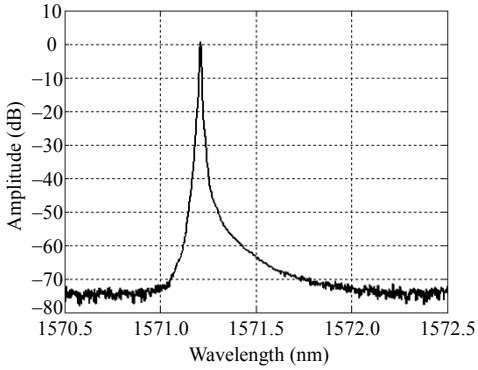

Fig. 4 Ultra-narrow laser linewidth obtained by a high resolution OSA at the output of the optical coupler.

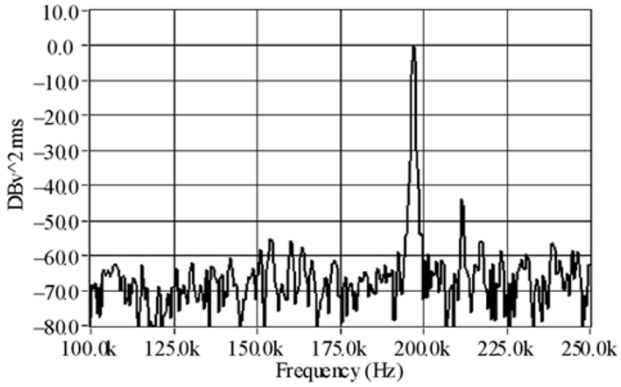

Fig. 5 FFT of the sensor's signal output when the ultrasound transducer was used to produce an acoustic wave in water at a frequency of 197 kHz (10-cm distance).

3. Results

In the experimental setup, a PZT 200LM450-ProWave was used as an acoustic source to simulate the pressure wave from a partial discharge. In underwater applications, the PZT had a transmitting sound pressure level of 155 dB (@ 0 dB ref 1 μPa/Vrms) with a central frequency of 200 kHz. The sensor signal was collected by a data acquisition (DAQ) board, and the further processing was done using the LabVIEW® software. At first, it was verified the signal stability when this laser sensor was working under acoustic excitation the erbium-doped fiber amplifier operation on the spectral width of the emission, the grating peak shift of the laser wavelength with the PS-CFBG response to the wave pressure and the correctness filtering of the CFBG pass-band and the correct operation of the detection system to compensate the temperature variations and maintain the interferometer locked at a quadrature point. Then, tests were done to evaluate the sensor response in the function of the distance, directionality and frequency.

3.1 Sensor resolution

The demodulation system noise level was $V_{\text{RMS-noise}}$= 0.1 mV, and the ultrasound transducer had a sound emitted pressure level of 320 Pa at 200 kHz. Tests were done at a distance of 10 cm (the standard distance for characterization of the acoustic emitter). The worst acoustic receiving sensitivity for the sensor was –200 dB (@ 0 dB = 1 Vrms/μPa) at the frequency of 250 kHz, which allowed a pressure resolution level of about 10 Pa.

3.2 Distance signal attenuation

The dependence on the distance of the sensor response was investigated. To evaluate the sensor performance in a situation close to the one present in power transformers, the sensing head was immersed in water and in oil. As can be observed in Fig. 6, the attenuation of the sensor output with the distance showed a similar behavior in all tests, with signal amplitude attenuations of 30 dB, 22 dB and 18 dB for air, water and oil-immersed cases, respectively, at a distance of 70 cm. Therefore, when compared with acoustic propagation in air, the results obtained for water and oil showed a stronger signal and a smaller

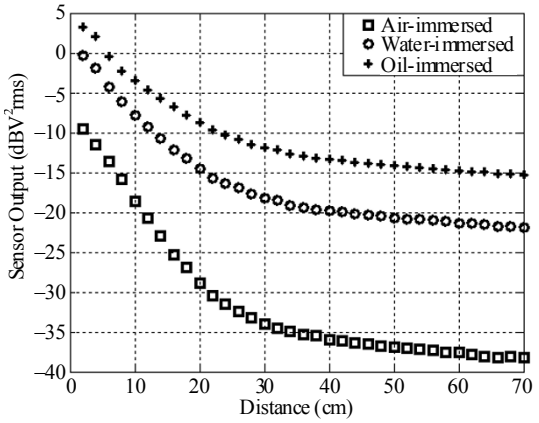

Fig. 6 Distance signal attenuation at the frequency of 100 kHz.

rate of signal attenuation with the distance, which were both positive features. This behavior was a consequence of the better acoustic energy transfer in a medium with a higher density. The results of the oil-immersed tests were particularly important to evaluate the sensor performance in view of the projected application.

3.3 Angular dependence

The normalized angular response for the sensor is shown in Fig. 7. The response of the sensor was collected for an angular orientation from 0º to 90º. The sensor directional aperture was defined by the angular range in which the normalized amplitude decreased to 0.5 (–3 dB) in reference to normal incidence. The directional apertures (φ angle in Fig. 2) for the sensor were about 60º at 10 kHz, 40º at 50 kHz, and 27º at 150 kHz. The directional aperture was important to determine the number of sensors and their spatial distribution in order to locate the discharge source by triangulation.

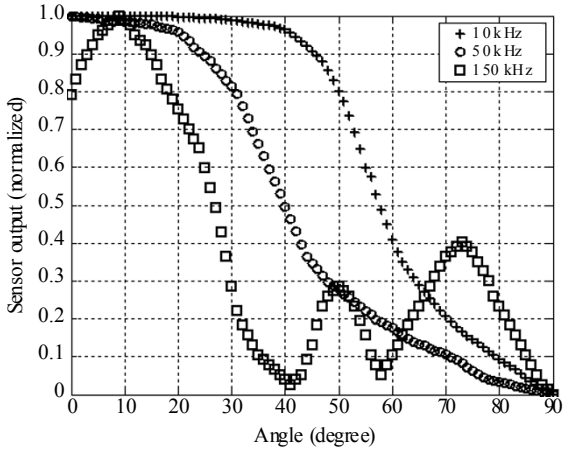

Fig. 7 Directionality of the sensor (angular response) in air at three different frequencies (10 kHz, 50 kHz, and 150 kHz).

3.4 Frequency response

The sensor frequency response depends basically on the mandrel's material (the Young modulus and Poisson ratio) and its geometry (radius, length and wall thickness). Figure 8(a) shows the mandrel frequency response in the frequency range of 0–250kHz that was obtained by the mathematical vibration model of the mandrel described in the preview section. A signal generator with flat response was used to drive the ultrasound transducer (emitter), and the frequency spectrum was also obtained experimentally. Figure 8(b) shows the sensor response when the frequency was swept from 1 kHz to 250 kHz. The sweep function needed 2 minutes to cover the entire frequency range, and the experiment was carried out during 20 min. Thus, the values in Fig. 6 are the means of 10 stored response values for each frequency. This experiment procedure explained the low smoothness of the response curve. A complex structure could be observed, certainly due to multiple resonances of the structure within this frequency window. The first modal resonance appeared at 45 kHz, a value close to the frequency resonance of the fundamental mode $f_{1,0}$ = 48.3 kHz (with n=0 and m=1) calculated by (4)

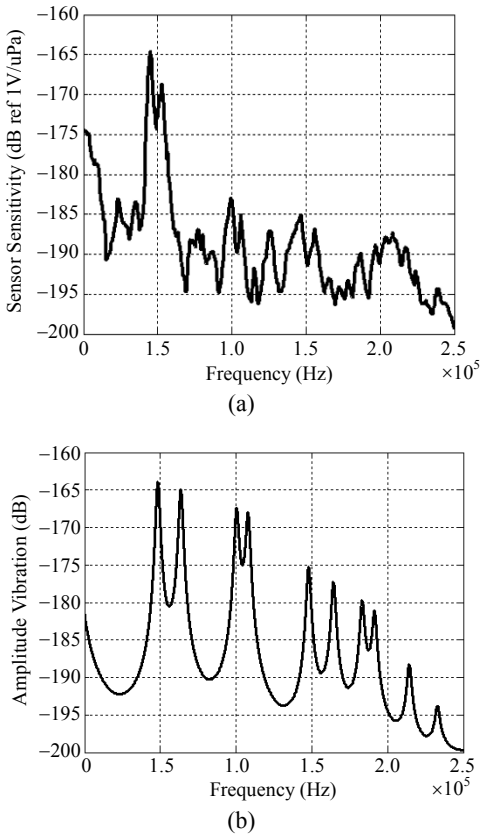

Fig. 8 Frequency response of the sensor in the frequency range of 0 – 250 kHz for (a) experimental and (b) simulated oil-immersed tests.

and using the correction factor given by (5) to oil-immersed tests, indicating a good agreement between the experimental data and the previsions derived from the mathematical vibration model of the mandrel. The sensor response was relatively flat (ripple of about 10 dB) in the range from 60 kHz to 230 kHz, but at higher frequencies the signal decreased dramatically (≈ 20 dB).

4. Conclusions

The primary motivation of this work was to demonstrate the feasibility of a new sensing concept for acoustic detection of partial discharges. The results obtained, in a perspective of "proof of concept", were promising and confirmed that partial discharge detector using a compact acoustic fiber sensor could be a better alternative to measurements taken from the exterior of the transformer (using e.g. piezoelectric transducers). The sensing system researched relied on a phase-shifted chirped fiber Bragg grating. The sensing element was attached to a compliant mandrel, and the sensor was interrogated by a processing interferometer incorporating active homodyne stabilization. A computer-based feedback loop was used to signal generation, acquisition and signal processing.

The results also showed that the proposed optical sensors, to be preferably mounted on the inside wall of the transformer tank (minimizing interference with the deployment of the electromagnetic field), presented an enhanced sensitivity and superior performance for acoustic detection of PD activity when compared to the conventional piezoelectric sensors externally mounted (high signal attenuation and reflections on the tank). The sensing system proposed could overcome this issue and increased dramatically the accuracy of the acoustic PDs location, considering it was able to detect directly the weak pressure disturbances produced by a PD activity and the acoustic signals could be separated from their reflections and the background noise by some methods of signal processing. Other advantages of the proposed PD detection and location system include: small size, high sensitivity, electrical nonconductivity and immunity to electro-magnetic interference (EMI).

Further work is necessary to reach a stage where the application of these sensors in power transformers becomes feasible. In particular, it is under study the effect of the mandrel geometry and material on the directionally of the acoustic detection and on the frequency response of the sensor. Additionally, the process and the materials for sensing head fabrication are being appropriately selected to support some harsh conditions (e.g. corrosive environment, high temperature, high static pressure), aiming to improve the achievable readout resolution. There are challenges to be faced to integrate a fiber sensing system into a power transformer, starting from the choice of the place inside the transformer where the sensors are to be deployed (windings, within the paper isolation, etc or preferably on the inner wall tank) to maximize acoustic capture and minimize electromagnetic field interference, which is theoretically expected to be minimal or negligible. This development, which hopefully will lead to not too expensive technological solutions, opens also a new path for condition monitoring and incipient fault analysis: the placement of a number of sensors inside the transformer tank will allow the construction of 3-dimensional acoustic images that will permit the pinpointing of sources of noise and eventually lead to more accurate diagnosis. Issues to be researched involve the long term sensor behavior in the complex inner environment of a power transformer (sensor life time, insulation degradation, insulation voids formation, hot spots influences, etc).

Acknowledgment

S. E. U Lima acknowledges the support of Fundação para a Ciência e a Tecnologia – FCT (Ph.D fellowship SFRH/BD/48724/2008).

References

[1] S. E. U. Lima, O. Frazão, R. G. Farias, F. M. Araújo, L. A. Ferreira, J. L. Santos, *et al*., "Mandrel-based fiber-optic sensors for acoustic detection of partial discharges – a proof of concept," *IEEE Transactions on Power Delivery*, vol. 25, no 4, pp. 2526–2534, 2010.

[2] V. Miranda and A. R. G. Castro, "Improving the IEC table for transformer failure diagnosis with knowledge extraction from neural networks," *IEEE Transactions on Power Delivery*, vol. 20, no. 4, pp. 2509–2516, 2005.

[3] T. Bengtsson, H. Kols, and B. Jönsson, "Transformer PD diagnosis using acoustic emission technique," presented at *10th Int. Symp. on High Voltage Engineering*, Montreal, Canada, Aug. 25–29, 1997.

[4] J. M. Lopez-Higuera, *Handbook of Optical Fiber Sensing Technology*. New York: John Wiley & Sons Inc., 2002.

[5] A. D. Kersey, "A review of recent developments in fiber optic sensor technology," *Optical Fiber Technology*, vol. 2, no. 3, pp. 291–317, 1996.

[6] K. P. Koo and A. D. Kersey, "Bragg grating-based laser sensors systems with interferometric interrogation and wavelength division multiplexing," *Journal of Lightwave Technology*, vol.13, no. 7, pp. 1243–1249, 1995.

[7] P. E. Bagnoli, N. Beverini, R. Falciai, E. Maccioni, M. Morganti, F. Sorrentino, *et al.*, "Development of an erbium-doped fiber laser as a deep-sea hydrophone," *Journal of Optics A: Pure and Applied Optics*, vol. 8, no. 7, pp. 535–539, 2006.

[8] P. E. Bagnoli, N. Beverini, B. Bouhadef, E. Castorina, E. Falchini, R. Falciai, *et al*, "Erbium-doped fiber lasers as deep-sea hydrophones," *Nuclear Instruments Methods in Physics Research Section A: Accelerators, Spectrometers, Detectors, Associated, Equipment*, vol. 567, no. 2, pp. 515–517, 2006.

[9] G. A. Ball and W. H. Glenn, "Design of a single-mode linear-cavity erbium fiber laser utilizing Bragg reflectors," *Journal of Lightwave Technology*, vol. 10, no. 10, pp. 1338–1343, 1992.

[10] A. D. Kersey, T. A. Berkoff, and W. W. Morey, "High-resolution fiber-grating based strain sensor with interferometric wavelength-shift detection," *Electronics Letters*, vol. 28, no. 3, pp. 236–238, 1992.

[11] Y. W. Song, S. A. Havstad, D. Starodubov, Y. Xie, A. E. Willner, and J. Feinberg, "40-nm-wide tunable fiber ring laser with single-mode operation using a highly stretchable FBG," *IEEE Photonics Technology Letters*, vol. 13, no. 11, pp. 1167–1169, 2001.

[12] S. H. Chang, I. K. Hwang, B. Y. Kim, and H. G. Park, "Widely tunable single-frequency Er-doped fiber laser with long linear cavity," *IEEE Photonics Technology Letters*, vol. 13, no. 4, pp. 287–289, 2001.

[13] X. Dong, N. Q. Ngo, P. Shum, H. Y. Tam, and X. Dong, "Linear cavity erbium-doped fiber laser with over 100 nm tuning range," *Optics Express*, vol. 11, no.14, pp. 1689–1694, 2003.

[14] D. Sabourdy, V. Kermene, A. Desfarges-Berthelemot, L. Lefort, A. Barthelemy, P. Even, *et al*., "Efficient coherent combining of widely tunable fiber lasers," *Optics Express*, vol. 11, no. 2, pp. 87–97, 2003.

[15] H. L. Liu, H. Y. Tam, W. H. Chung, P. K. A. Wai, and N. Sugimoto, "Low beat-noise polarized tunable fiber ring laser," *IEEE Photonics Technology Letters*, vol. 18, no. 5, pp. 706–708, 2006.

[16] S. Y. Li, N. Q. Ngo, and Z. R. Zhang, "Tunable fiber laser with ultra-narrow linewidth using a tunable phase-shifted chirped fiber grating," *IEEE Photonics Technology Letters*, vol. 20, no. 17, pp. 1482–1484, 2008.

[17] T. Bengtsson, M. Leijon, and L. Ming, "Acoustic frequencies emitted by partial discharges in oil," presented at *8th Int. Symp. on High Voltage Engineering*, Yokohama, Japan, Aug. 22–27, 1993.

[18] T. Krauthammer and E. Ventsel, *Thin plates and shells: theory, analysis and applications*, 1st ed. New York: Mercel Dekker Inc., 2001.

[19] W. Soedel, *Vibrations of Shells and Plates*, 3rd ed. New York: Mercel Dekker Inc., 2004.

[20] M. Anghinolfi, A. Calvi, A. Cotrufo, M. Ivaldi, O. Yershova, F. Parodi, *et al*., "A fiber optic air backed mandrel hydrophone to detect high energy hadronic showers in the Water," presented at *Workshop of the Russian-Italian collaboration in the Cosmic Ray Physics*, Moscow, Oct. 17, pp. 1–9, 2005.